Crimson Publishers
Wings to the Research

Research Article

Evaluation of the Structural Properties and Isotopic Abundance Ratios of Consciousness Energy Treated Pyridoxine Using LC-MS, GC-MS, and NMR Spectroscopy

Mahendra Kumar Trivedi[1] and Snehasis Jana[2]*

[1]Trivedi Global, Inc, Henderson, Nevada, USA

[2]Trivedi Science Research Laboratory Pvt Ltd, Thane (W), India

ISSN: 2637-7802

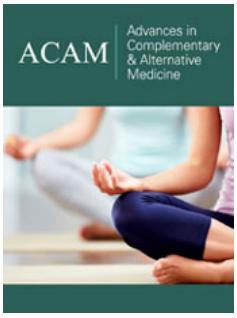

***Corresponding author:** Snehasis Jana, Trivedi Science Research Laboratory Pvt Ltd, Thane (W), India

Submission: March 04, 2020

Published: March 10, 2020

Volume 6 - Issue 1

How to cite this article: Mahendra Kumar Trivedi, Snehasis Jana. Evaluation of the Structural Properties and Isotopic Abundance Ratios of Consciousness Energy Treated Pyridoxine Using LC-MS, GC-MS, and NMR Spectroscopy. Adv Complement Alt Med. 6(1). ACAM.000629.2020.
DOI: 10.31031/ACAM.2020.06.000629

Abstract

Pyridoxine (vitamin B_6) is an essential water-soluble vitamin widely used in nutraceutical and pharmaceutical formulations for the prevention and treatment of vitamin B_6 deficiency and other diseases. The objective of the study was to explore the impact of the Trivedi Effect®-Consciousness Energy Treatment on the isotopic abundance ratios and structural properties of pyridoxine hydrochloride using LC-MS, GC-MS, and NMR analytical techniques. The pyridoxine sample was equally divided into control/ untreated and Biofield Energy Treated pyridoxine. The treated pyridoxine sample received Biofield Energy Treatment (the Trivedi Effect®) remotely for ~3 minutes by Mr. Mahendra Kumar Trivedi, who was located in the USA, while the test samples were located in the research laboratory in India. The treated sample was designated as the Biofield Energy Treated sample. The LC-ESI-MS analysis of both of the pyridoxine samples showed the protonated parent ion mass at *m/z* 170 (calcd for $C_8H_{12}NO_3^+$, 170.08) at retention times (R_t) 2.41 minutes. But, the relative peak intensities of the treated pyridoxine were significantly improved compared to the control sample. The isotopic abundance ratios of P_{M+1}/P_M ($^2H/^1H$ or $^{13}C/^{12}C$ or $^{15}N/^{14}N$ or $^{17}O/^{16}O$) and P_{M+2}/P_M ($^{18}O/^{16}O$) were significantly increased by 11.92% and 153.85%, respectively in the treated pyridoxine compared to the control sample. Thus, ^2H, ^{13}C, ^2H, ^{15}N, ^{17}O contributions from $C_8H_{12}NO_3^+$ to the isotopic *m/z* 171 and ^{18}O contribution to the isotopic *m/z* 172 was significantly increased in the treated sample compared with the control sample. The GC chromatographic peak area% and GC-MS mass peak intensity of the treated sample was significantly increased by 15.88% and 32.26%, respectively compared to the control sample. The proton and carbon signals for CH_3, CH_2, NH_2, CH, =C=, and C-OH groups in the ^1H and ^{13}C NMR spectra of the control and treated samples were similar. The increased mass peak intensities, peak area%, and isotopic abundance ratios in the Biofield Energy Treated pyridoxine might be the impact of the Trivedi Effect®-Consciousness Energy Treatment via the possible mediation of neutrinos, which further lead to the change in the kinetic isotope effects of the treated pyridoxine. Thus, the Trivedi Effect® Treated pyridoxine might be advantageous for designing better nutraceutical, dietary supplements and/or pharmaceutical formulations which might provide better therapeutic response against vitamin B_6 deficiency, hereditary sideroblastic anemia, premenstrual syndrome, cardiovascular disease, pyridoxine-dependency seizures, febrile seizures, pulmonary tuberculosis, metabolic disorders, Alzheimer's disease, cancer, hyperhomocysteinemia, anxiety, asthma, depression, attention deficit hyperactivity disorder, dysmenorrhea, akathisia, angioplasty, birth outcomes, cognitive function, hyperkinetic cerebral dysfunction syndrome, carpal tunnel syndrome, hypertension, immune system function, breast pain, pregnancy-induced nausea and vomiting, lactation suppression, McArdle's disease, osteoporosis, Tardive dyskinesia, autism, stroke recurrence, etc.

Keywords: Pyridoxine; The Trivedi Effect®; Energy of Consciousness Treatment; LC-MS; Isotopic abundance; Kinetic isotope effects; GC-MS

Introduction

Pyridoxine (pyridoxol/vitamin B_6) is a water-soluble vitamin widely distributed in food and dietary supplements [1]. It occurs naturally in foods such as chickpeas, fish, meat, poultry, nuts, whole grains, bananas, spinach, tofu, avocados, etc. [2] It usually acts like a cofactor or prosthetic group for more than 100 enzymatic reactions. Pyridoxal 5' phosphate (PLP) and pyridoxamine 5' phosphate (PMP) are involved in the metabolism of amino acids, carbohydrates, and lipids. Pyridoxine also plays important role in biosynthesis of neurotransmitters and maintaining normal levels of homocysteine, amino acid in the blood, gluconeogenesis, glycogenolysis, immune function (lymphocyte and interleukin-2 production), and hemoglobin formation

[3-5]. Pyridoxine hydrochloride is the commonly used salt form of vitamin B_6 [6]. Vitamin B_6 is generally used as vitamin supplement and also as a component of multivitamin preparations for the prevention and treatment of vitamin B_6 deficiency, sideroblastic anaemia, metabolic disorder, cardiovascular disease, Alzheimer's disease, pyridoxine-dependent epilepsy, pulmonary tuberculosis, hyperhomocysteinaemia, cancer, anxiety, asthma, depression, attention deficit hyperactivity disorder (ADHD), dysmenorrhoea, diabetes, post-partum lactation suppression, McArdle's disease, osteoporosis, problems from isoniazid, mushroom poisoning, etc. [1,3-8]. Vitamin B_6 seldom shows side-effects like headache, sleepiness, numbness, sensory neuropathy (ataxia), etc. It can interact with many medications, i.e., cycloserine, antiepileptic drugs (valproic acid, carbamazepine, phenytoin, etc.), theophylline, etc. might adversely affect vitamin B_6 levels [3,5].

There is a quantum energy matrix that surrounds the human body resulting from the continuous movement of the electrically charged particles (ions, cells, etc.) inside the body is called the Biofield Energy [9,10]. Biofield Energy Practitioners have the ability to harness the inherently intelligent energy from the "universal energy field" and can transmit into any living or nonliving object(s) anywhere on the planet. Biofield based Energy Therapies are used against various human disease conditions and accepted in many countries [11,12]. Biofield Energy Healing therapy has been recognized as a Complementary and Alternative Medicine (CAM) health care approach by National Center of Complementary and Integrative Health (NCCIH) with other therapies, medicines and practices such as yoga, Ayurvedic medicine, traditional Chinese herbs and medicines, aromatherapy, Reiki, cranial sacral therapy, Qi Gong, Tai Chi, chiropractic/osteopathic manipulation, meditation, homeopathy, acupressure, acupuncture, healing touch, hypnotherapy, movement therapy, naturopathy, etc. [13,14]. The Trivedi Effect® is natural and only scientifically proven phenomenon [15]. The Trivedi Effect®-Biofield Energy Treatment is significantly drawing attention in several fields include materials science [16,17], nutraceuticals [18,19], pharmaceuticals [20,21], organic compounds [22,23], microbiology [24,25], agricultural [26,27], biotechnology [28], medical [29] due to its astounding ability for modification of the characteristic properties. Some of the literature has reported significant problems about the bioavailability of vitamin B_6 due to the very limited extent intestinal absorption of B_6 vitamers, large rate of elimination due to the non-binding properties of pyridoxine to the proteins of blood plasma, instability of pyridoxine due to the complex formation between various food, drug, and food stored at elevated temperatures [4,6,30,31]. The recent study of the Trivedi Effect®-Consciousness Energy Treatment on the pharmaceutical/nutraceutical compounds, i.e., resveratrol, berberine, and 25-hydroxyvitamin D_3 reported significant improvement of the bioavailability in Male Sprague-Dawley rats [32-34]. These effects of the Energy of Consciousness Treatment (the Trivedi Effect®) are proposed to act through the possible mediation of neutrinos [15,32-34].

The analysis of stable isotope ratios (e.g., C,H,O,N,S,Fe,Ca,Cu,S, etc.) can provide powerful tracers and chronometers for anthropology, geosciences, archaeology, environmental studies, and health research [35-39]. Highly sophisticated analytical instruments like Gas chromatography – mass spectrometry (GC-MS) and liquid chromatography - mass spectrometry (LC-MS) techniques are widely used for the study of isotope ratio analysis with sufficient precision [38]. So many studies have been performed to evaluate the impact of the Trivedi Effect® on the isotopic abundance ratios of organic compounds, and the significant alteration of the isotopic abundance ratio of the organic compounds were reported due to the Trivedi Effect® [22,23]. Thus, the current study has been designed to evaluate influence of the Trivedi Effect®-Consciousness Energy Treatment on the isotopic abundance ratios P_{M+1}/P_M ($^2H/^1H$ or $^{13}C/^{12}C$ or $^{15}N/^{14}N$ or $^{17}O/^{16}O$) and P_{M+2}/P_M ($^{18}O/^{16}O$) and structural properties of pyridoxine HCl using LC-MS, GC-MS, and NMR (Nuclear Magnetic Resonance) analytical techniques.

Materials and Methods

Chemicals and reagents

Pyridoxine hydrochloride ($C_8H_{12}ClNO_3$; 100%) was purchased from TCI, Japan. All other chemicals used during the experiments were of analytical grade available in India.

Consciousness energy healing treatment strategies

The pyridoxine hydrochloride sample was divided into two parts. One part of the pyridoxine was considered as control/untreated, which was not treated with the Biofield Energy Treatment. The second part of the pyridoxine sample was treated with the Trivedi Effect®-Consciousness Energy Treatment remotely under standard laboratory conditions for ~3 minutes by Mr. Mahendra Kumar Trivedi and termed as the Biofield Energy Treated/the Trivedi Effect® Treated pyridoxine. Trivedi was located in the USA, while the test samples were located in the research laboratory in India. This Biofield Energy Treatment was provided through the Mahendra Trivedi's unique energy transmission process to the test item. Further, the control sample was treated by a "sham" healer for better comparison. The sham healer did not have any knowledge about the Biofield Energy Treatment. The Biofield Energy Treated and untreated samples of pyridoxine were kept in sealed conditions and characterized using LC-MS, GC-MS, and NMR techniques.

Characterization

Liquid chromatography-mass spectrometry (LC-MS) analysis and Calculation of Isotopic Abundance Ratio: The LC-MS analysis of the control and Biofield Energy Treated pyridoxine was performed using LC-Dionex Ultimate 3000, MS-TSQ Endura, (USA) equipped with a photo-diode array (PDA) detector connected with a triple-stage quadrupole mass spectrometer (Thermo Scientific TSQ Endura, USA) with a Thermo Scientific Ion Max NG source and atmospheric pressure chemical ionization (APCI). The

analysis was performed on a reversed phase Zorbax Eclipse-C18 100 × 4.6mm, 3.5µm in isocratic mode (A: B-75:25v/v) in the liquid chromatograph. The mobile phase was 0.1% formic acid in water (mobile phase A), and acetonitrile (mobile phase B) at a constant flow rate of 0.5mL/min. The column temperature was kept constant at 35 °C. The injection volume was 5µL and the total run time was 15 minutes. Peaks were monitored using the PDA (295nm) detector. Mass spectrometric analysis was performed under +ve ESI mode. The total ion chromatogram, peak area% and mass spectrum of the individual peak which appeared in LC along with the full scan were recorded. The mass peak intensities of the mass spectrum of the individual peak were recorded.

The natural abundance of C, O, N, and H isotope can be predicted from the comparison of the relative abundance of the isotope peak with respect to the base peak. The values of the natural isotopic abundance of the common elements are obtained from the literature [39-42]. The isotopic abundance ratios (P_{M+1}/P_M and P_{M+2}/P_M) for the control and Biofield Energy Treated pyridoxine were calculated.

Percentage (%) change in isotopic abundance ratio of pyridoxine = $[(IAR_{Treated} - IAR_{Control})/ IAR_{Control}) \times 100]$

Where, $IAR_{Treated}$: isotopic abundance ratio in the treated pyridoxine and $IAR_{Control}$: isotopic abundance ratio in the control pyridoxine.

Gas chromatography-mass spectrometry (GC-MS) analysis: The GC-MS analysis of the control and the Biofield Energy Treated pyridoxine was performed using Agilent 7890B Gas chromatograph equipped with a silica capillary column HP-5 MS (30m x 0.25mm x 0.25µm) and coupled to a quadrupole detector with pre-filter (5977B, USA) was operated with electron impact (EI) ionization in positive ion mode at 70eV. Oven temperature was programmed from 80 °C (1 min hold) to 200 °C@ 10 °C/min (5min hold) to 300 °C (2min hold) @20 °C/min. Temperatures of the injector, detector (FID), auxiliary, ion source, and quadrupole detector were 250, 260, 280, 230, and 150 °C. Pyridoxine HCl was dissolved in methanol, and 1.0µL was splitlessly injected with helium as a carrier gas with a flow rate of 2.0mL/min. Mass spectra were scanned from *m/z* 40 to 1050 at a stability of ±0.1*m/z* mass accuracy over 48 hours and mass peak intensities of the mass spectrum of the individual peak were recorded.

Percent change in peak intensity (I) was calculated using following equations:

$$\text{Percentage change in peak intensity(I)} = \frac{[I_{Treated} - I_{Control}]}{I_{Control}} \times 100$$

Where, $I_{Control}$ and $I_{Treated}$ are the peak intensity of the control and the Biofield Energy Treated samples, respectively.

Nuclear magnetic resonance (NMR) analysis: 1H NMR spectra of pyridoxine HCl were recorded at 400MHz on Agilent-MRDD2 FT-NMR. Approximately 3mg of the sample was dissolved in DMSO-d6. Chemical shifts (d) were in parts per million (ppm) relative to the solvent's residual proton chemical shift $\{(CD_3)_2SO, \delta = 2.5\}$. ^1H NMR multiplicities were designated as singlet (s), doublet (d), doublet of doublet (dd), triplet (t), quartet (q), multiplet (m), broad (br), apparent (app). Similarly, ^{13}C NMR spectra of pyridoxine HCl were measured at 100MHz on Agilent-MRDD2 FT-NMR spectrometer at room temperature. Approximately 25mg of the sample was dissolved in DMSO-d6. Chemical shifts (d) were in parts per million (ppm) relative to the solvent's residual carbon chemical shift $\{(CD_3)_2SO, \delta = 39.52\}$.

Results and Discussion

Liquid chromatography-mass spectrometry (LC-MS) analysis

The control and the Biofield Energy Treated pyridoxine HCl showed a clear and sharp peak at retention times (R_t) 2.4 minutes in both the chromatograms (Figure 1). The peak area% of the control and the Biofield Energy Treated pyridoxine at R_t 2.4 minutes was 99.99 in case of both control and the Biofield Energy Treated pyridoxine. The peak area% of the Biofield Energy Treated sample was similar to the control sample, which indicated that the polarity of both the samples was similar.

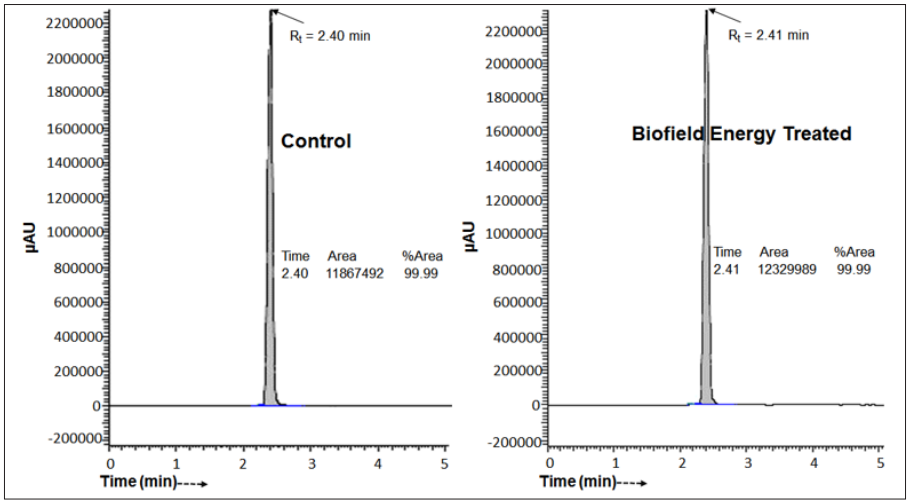

Figure 1: Total ion chromatograms (TIC) of the control and Biofield Energy Treated pyridoxine HCl.

The ESI-MS spectra of the control pyridoxine exhibited the protonated molecular ion mass peak (Figure 2) at *m/z* 170.02 (calcd for $C_8H_{12}NO_3^+$, 170.08). Similarly, the mass spectra of the Biofield Energy Treated pyridoxine exhibited the protonated molecular ion mass peak (Figure 2) at *m/z* 170.05 (calcd for $C_8H_{12}NO_3^+$, 170.08). The parent mass peak at *m/z* 170 was the base peak which exhibited 100% relative abundance in both the spectra (Figure 2). Although the fragmentation patterns of the control and the Biofield Energy Treated pyridoxine were similar, the relative peak intensities of the Biofield Energy Treated pyridoxine were significantly improved compared to the control sample.

Isotopic abundance ratio analysis

The control and the Biofield Energy Treated samples of pyridoxine showed the protonated molecular ion mass peak at *m/z* 170.02 (calcd for $C_8H_{12}NO_3^+$, 170.08) with 100% relative abundance in the mass spectra. The theoretical calculation of isotopic peak P_{M+1} for the protonated pyridoxine presented below:

P (^{13}C) = [(8 x 1.1%) x 100% (the actual size of the M^+ peak)] / 100% = 8.8%

P (^{2}H) = [(12 x 0.015%) x 100%] / 100% = 0.18%

P (^{15}N) = [(1 x 0.40%) x 100%] / 100% = 0.4%

P (^{17}O) = [(3 x 0.04%) x 100%] / 100% = 0.12%

P_{M+1} i. e.^{13}C, ^{2}H, ^{15}N, and ^{17}O contributions from $C_8H_{12}NO_3^+$ to *m/z* 171 = 9.5%

Similarly, the theoretical calculation of isotopic peak P_{M+2} for the protonated pyridoxine presented below:

P (^{18}O) = [(3 x 0.20%) x 100%] / 100% = 0.6%

P_{M+2} of 18O contribution from $C_8H_{12}NO_3$+ to *m/z* 172 = 0.6%

The calculated isotopic abundance of P_{M+1} and P_{M+2} values were near to the observed values (Table 1). The probability of A + 1 and A + 2 elements having an isotope with one and two mass unit heavier, respectively than the most abundant isotope (i.e., ^{13}C, ^{15}N, ^{17}O, and ^{18}O) contributions to the mass of the isotopic molecular ion $[M+1]^+$ and $[M+2]^+$. ^{2}H did not contribute much any isotopic *m/z* ratios because of its less natural abundance compared to the abundances of C, N, and O isotopes [40-43]. But, the contributions of ^{13}C, ^{15}N, ^{17}O, and ^{18}O was major from pyridoxine to the isotopic mass peak at *m/z* 171 and 172 confirmed from the calculations. Therefore, P_M, P_{M+1}, and P_{M+2} of the pyridoxine at *m/z* 170, 171, and 172 of the control and Biofield Energy Treated samples were obtained from the experimental relative abundance of M^+, $(M+1)^+$, and $(M+2)^+$ peaks, respectively in the mass spectra (Figure 2 and Table 1).

Table 1: LC-ESI-MS isotopic abundance ratio analysis of control and Biofield Energy Treated pyridoxine.

Parameter	Control Sample	Biofield Energy Treated Sample
P_M at *m/z* 170 (%)	100	100
P_{M+1} at *m/z* 171 (%)	6.29	7.04
P_{M+1}/P_M	0.0629	0.0704
% Change of isotopic abundance ratio (P_{M+1}/P_M) with respect to the control pyridoxine		11.92
P_{M+2} at *m/z* 172 (%)	0.13	0.33
P_{M+2}/P_M	0.0013	0.0033
% Change of isotopic abundance ratio (P_{M+2}/P_M) with respect to the control pyridoxine		153.85

P_M = the relative peak intensity of the parent molecular ion M^+; P_{M+1} = the relative peak intensity of the isotopic molecular ion $[M+1]^+$, P_{M+2} = the relative peak intensity of the isotopic molecular ion $[M+2]^+$, and M = mass of the parent pyridoxi

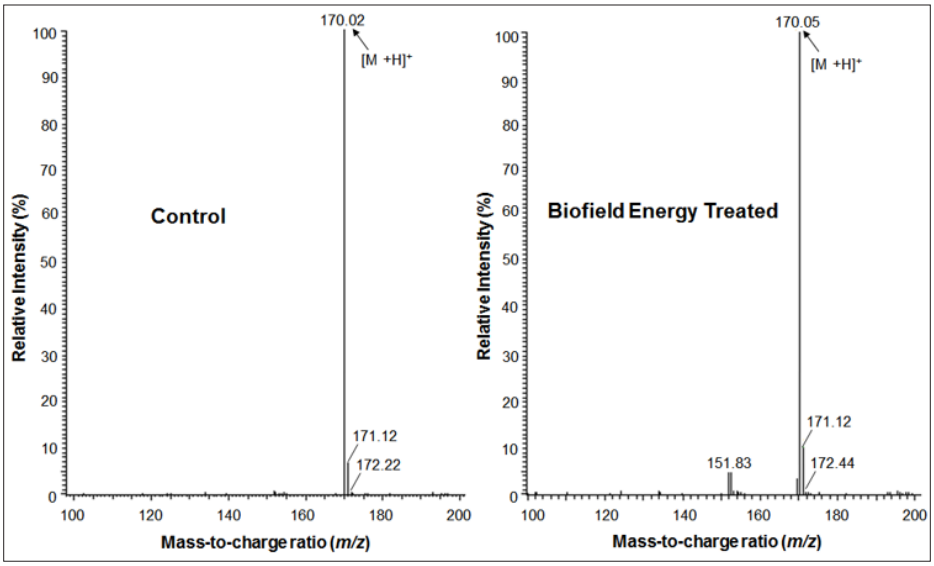

Figure 2: The ESI-MS spectra of the control and the Biofield Energy Treated pyridoxine at R_t 2.4 minutes in the chromatograms.

Table 1 summarized the percentage change in the isotopic abundance ratios (P_{M+1}/P_M and P_{M+2}/P_M) in the Biofield Energy Treated pyridoxine compared to the control sample. The isotopic abundance ratio of P_{M+1}/P_M ($^2H/^1H$ or $^{13}C/^{12}C$ or $^{15}N/^{14}N$ or $^{17}O/^{16}O$) in the Biofield Energy Treated pyridoxine was increased by 11.92% compared to the control sample (Table 1). This indicated that the ^2H, ^{13}C, ^2H, ^{15}N, and ^{17}O contributions from $C_8H_{12}NO_3^+$ to the isotopic *m/z* 171 in the Biofield Energy Treated pyridoxine sample was significantly increased compared to the control sample. Correspondingly, the isotopic abundance ratio of P_{M+2}/P_M ($^{18}O/^{16}O$) in the Biofield Energy Treated pyridoxine also significantly increased by 153.85% compared to the control sample (Table 1). Therefore, the ^{18}O contribution from $C_8H_{12}NO_3^+$ to the isotopic *m/z* 172 in the Biofield Energy Treated pyridoxine was significantly increased compared to the control sample.

The significant improvement of the isotopic abundance ratios (P_{M+1}/P_M and P_{M+2}/P_M) might be the impact of the Trivedi Effect®-Consciousness Energy Treatment which purports to provide the necessary energy for the neutrino oscillations which leads to the alteration of the fundamental properties of any subject(s) [15,22,23]. The neutrino oscillations seem to give credence to the postulates of researchers on the Trivedi Effect® [15]. A neutrino is an electrically neutral elementary particle with negligible unit mass, interacts only via the weak subatomic force and gravity [44,45]. Alteration in atomic/molecular level postulated to the changes in atomic mass and charge through the possible mediation of neutrinos [15,46-48]. The altered isotopic abundance ratio leads to the alteration of the kinetic isotope effects of the atoms/molecules. This is very useful to study the reaction mechanism, understand the enzymatic transition state, and enzyme mechanism, which is supportive to design effective and specific inhibitors, etc. [39]. Therefore, the Biofield Energy Treated pyridoxine with altered isotopic abundance ratios was assumed to be more advantageous for the designing of better nutraceutical/ pharmaceutical formulations.

Gas chromatography-mass spectrometry (GC-MS) analysis

The GC-MS chromatograms of the control and the Biofield Energy Treated samples of pyridoxine are shown in Figure 3. Both the chromatograms showed a similar type of chromatographic peaks with similar R_t. The retention times of pyridoxine was found at 13.8 minutes in both the chromatograms of control and the Biofield Energy Treated samples. This indicated that the polarity of the control and the Biofield Energy Treated pyridoxine is same. But, the GC chromatographic peak area% of the Biofield Energy Treated pyridoxine (70.21%) was significantly increased by 15.88% compared to the control sample (60.59%) (Table 2). This indicated that the solubility of the Biofield Energy Treated pyridoxine was increased compared to the control sample.

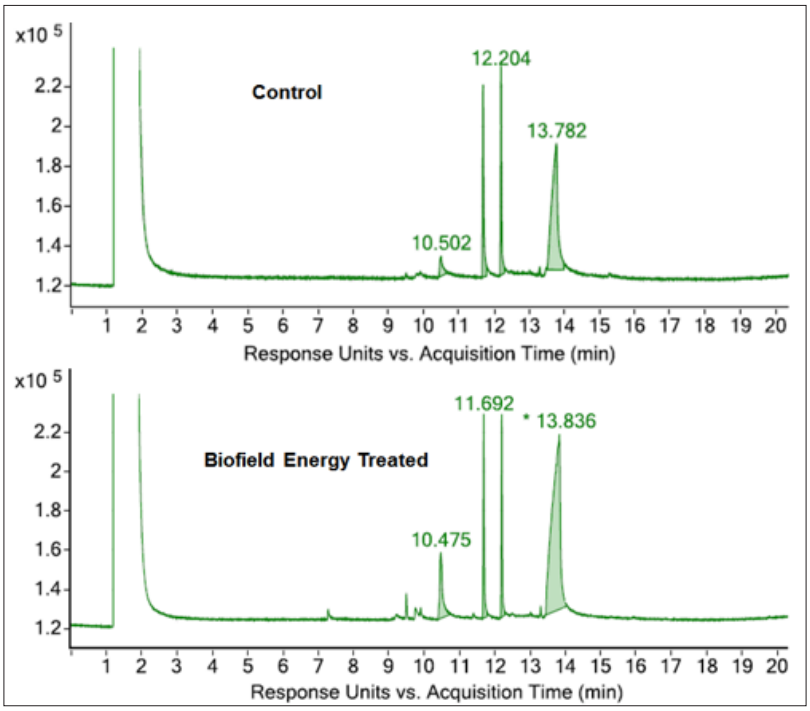

Figure 3: GC chromatograms of the control and Biofield Energy Treated pyridoxine HCl.

The GC-MS spectra of the control and Biofield Energy Treated pyridoxine at R_t of 13.8 minutes exhibited the presence of the molecular ion (Figure 4) at *m/z* 169.1 (calcd for $C_8H_{11}NO_3^+$, 169.07). The other mass fragmentation peak at lower *m/z* 151.1, 136.0, 122.1, 106.1, and 94.1 corresponded to the molecular formula $C_8H_9NO_2^{\bullet+}$, $C_8H_{10}NO^+$, $C_7H_8NO^+$, $C_7H_8N^+$, and $C_6H_8N^+$, respectively were observed in both control and the Biofield Energy Treated pyridoxine (Figures 4 & 5). The mass fragmentation patterns of the

Biofield Energy Treated pyridoxine were similar compared to the control sample. But the mass peak intensities of the Biofield Energy Treated pyridoxine were significantly altered compared to the control pyridoxine. The mass peak intensity of the control and the Biofield Energy Treated pyridoxine were 62965.86 and 83278.98, respectively at R_t 13.8 minutes. The mass peak intensity of the Biofield Energy Treated pyridoxine was significantly increased by 32.26% compared to the control pyridoxine (Table 2). The improved mass peak intensities were assumed to be the influence of the Trivedi Effect®-Consciousness Energy Treatment [15,22,23].

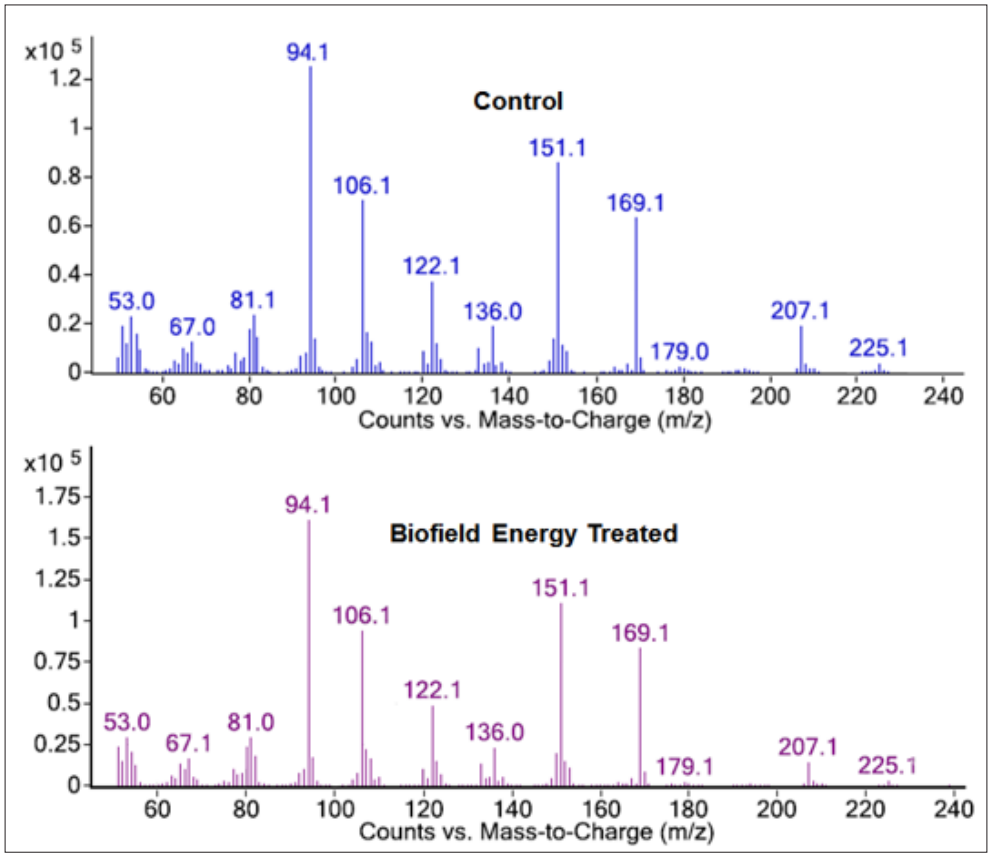

Figure 4: GC-MS spectra of the control and Biofield Energy Treated pyridoxine at R_t 13.8 minutes.

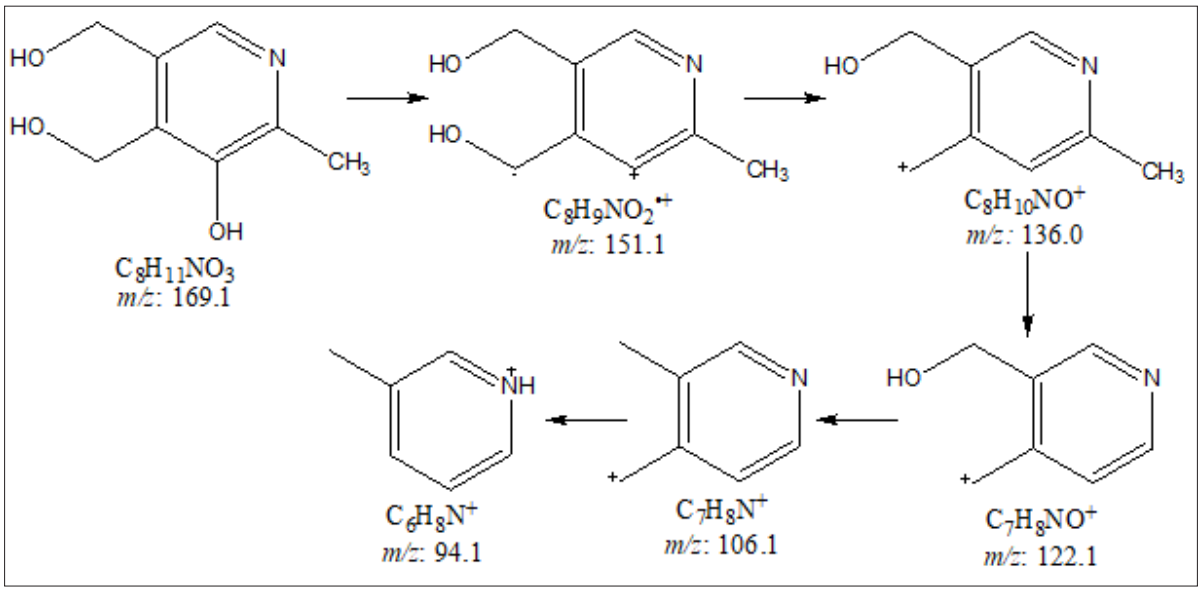

Figure 5: Proposed fragmentation pathway of pyridoxine.

Table 2: GC-MS chromatographic and mass spectra analysis at R_t 13.8 minutes of the control and the Biofield Energy Treated pyridoxine.

Parameters	Control sample	Biofield Energy Treated sample	% Change
Peak area%	60.59	70.21	15.88
Mass peak (*m/z* = 169.1) intensity	62965.86	83278.98	32.26

Nuclear magnetic resonance (NMR) spectroscopy analysis

^{1}H spectra of the control and the Biofield Energy Treated pyridoxine are shown in Figure 6. The signals for the protons coupling of CH_3, CH_2, CH, and OH protons in both the ^{1}H NMR spectra of pyridoxine were in the range of δ 2.59 to 16.03ppm (Table 3). The proton signals of the Biofield Energy Treated pyridoxine were close to the control sample. The 13C NMR spectra of the control and the Biofield Energy Treated pyridoxine are shown in Figure 7. The carbon signals for CH_3, CH_2, CH, =C=, and C-OH groups in both the control and the Biofield Energy Treated ^{13}C NMR spectra were in the range of 14.7-151.89 (Table 3). The experimental data closely matched to the published literature [49,50]. The ^{1}H and ^{13}C NMR results indicated that there was no structural modification of the Biofield Energy Treated pyridoxine compared to the control sample.

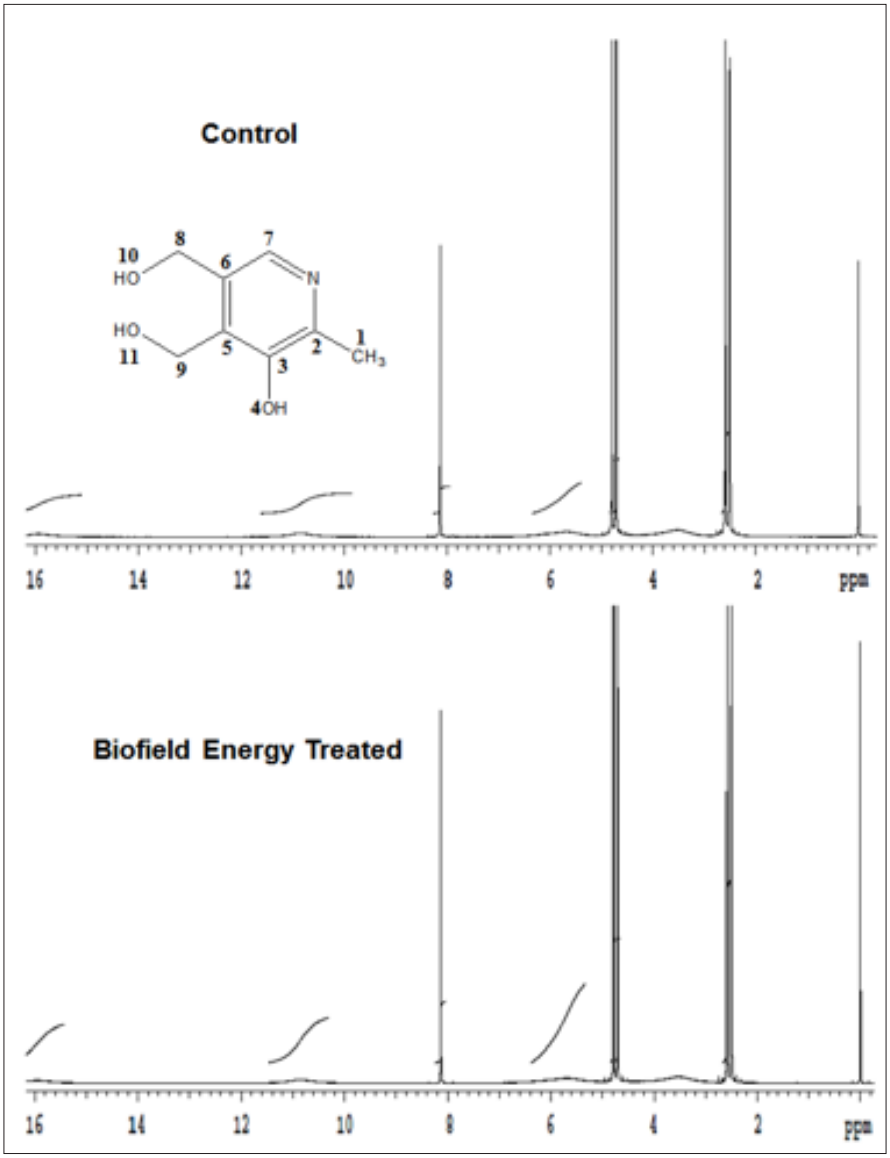

Figure 6: The ^{1}H NMR spectra of the control and Biofield Energy Treated pyridoxine.

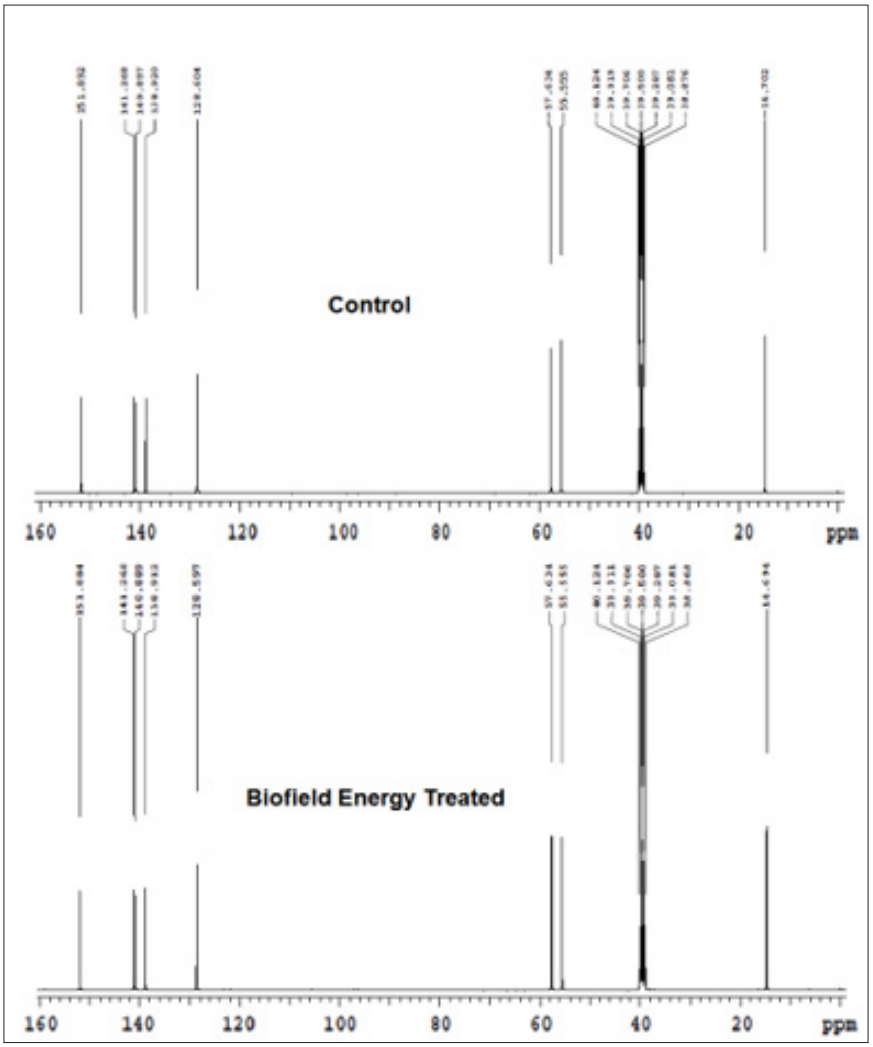

Figure 7: The ^{13}C NMR spectra of the control and Biofield Energy Treated pyridoxine.

Table 3: ^{1}H and ^{13}C NMR spectroscopic data of both the control and Biofield Energy Treated pyridoxine.

^{1}H & ^{13}C S. No	^{1}H NMR δ (ppm) & Multiplicity		^{13}C NMR δ (ppm)	
	Untreated	Biofield Energy Treated	Untreated	Biofield Energy Treated
1	2.59 (S, 3H)	2.59 (S, 3H)	14.702	14.69
2	--	--	141.26	141.26
3	--	--	151.89	151.88
4	5.67 (b, H)	5.66 (b, H)	--	--
5	--	--	138.92	138.9
6	--	--	140.89	140.88
7	8.13 (s, H)	8.13 (s, H)	128.62	128.6
8	4.70 (s, 2H)	4.70 (s, 2H)	57.67	57.5
9	4.78 (s, 2H)	4.78 (s, 2H)	55.65	55.62
10	10.85 (b, H)	10.83 (b, H)	--	--
11	16.03 (b, H)	15.99 (b, H)	--	--

s: singlet; b: broad.

Conclusion

The Trivedi Effect®-Consciousness Energy Treatment on pyridoxine by Mr. Mahendra Kumar Trivedi showed an astounding significant impact on the relative peak intensities, peak area%, and isotopic abundance ratios. The LC-ESI-MS analysis of both the control and the Biofield Energy Treated pyridoxine samples showed the protonated parent ion mass at *m/z* 170 (calcd for $C_8H_{12}NO_3^+$, 170.08) at retention times (R_t) 2.41 minutes. But, the relative peak intensities of the Biofield Energy Treated pyridoxine were significantly improved compared to the control sample. The isotopic abundance ratios of P_{M+1}/P_M ($^2H/^1H$ or $^{13}C/^{12}C$ or $^{15}N/^{14}N$ or $^{17}O/^{16}O$) and P_{M+2}/P_M ($^{18}O/^{16}O$) were significantly increased by 11.92% and 153.85%, respectively in the Biofield Energy Treated pyridoxine compared to the control sample. Thus, ^2H, ^{13}C, ^2H, ^{15}N, ^{17}O contributions from $C_8H_{12}NO_3^+$ to the isotopic *m/z* 171 and ^{18}O contribution to the isotopic *m/z* 172 significantly increased in the Biofield Energy Treated sample compared with the control sample. The GC chromatographic peak area% and GC-MS mass peak intensity of the Biofield Energy Treated sample significantly increased by 15.88% and 32.26%, respectively compared to the control sample. The proton and carbon signals for CH_3, CH_2, NH_2, CH, =C=, and C-OH groups in the ^1H and ^{13}C NMR spectra of the control and the Biofield Energy Treated samples were similar. The increased mass peak intensities, peak area%, and isotopic abundance ratios in the Biofield Energy Treated pyridoxine might be the impact of the Trivedi Effect®-Consciousness Energy Treatment via the possible mediation of neutrinos, which further lead to the change in the kinetic isotope effects of the Biofield Energy Treated pyridoxine. Thus, the Trivedi Effect® Treated pyridoxine could be advantageous for designing better nutraceutical, dietary supplements and/or pharmaceutical formulations which might provide better therapeutic response against vitamin B_6 deficiency, hereditary sideroblastic anemia, premenstrual syndrome, cardiovascular disease, pyridoxine-dependency seizures, febrile seizures, pulmonary tuberculosis, metabolic disorders, Alzheimer's disease, cancer, hyperhomocysteinemia, anxiety, asthma, depression, attention deficit hyperactivity disorder (ADHD), dysmenorrhea, akathisia, angioplasty, birth outcomes, cognitive function, hyperkinetic cerebral dysfunction syndrome, carpal tunnel syndrome, hypertension, immune system function, McArdle's disease, osteoporosis, lactation suppression, pregnancy-induced nausea and vomiting, breast pain, Tardive dyskinesia, autism, stroke recurrence, problems from isoniazid, mushroom poisoning, etc.

Acknowledgement

The authors are grateful to GVK Biosciences Pvt. Ltd., Trivedi Science, Trivedi Global, Inc., and Trivedi Master Wellness for their assistance and support during this work.

References

1. WHO Model Formulary (2008) World Health Organization. 2009: 496.
2. US Department of Agriculture, Agricultural Research Service (2011) USDA National Nutrient Database for Standard Reference, Release 24.
3. https://ods.od.nih.gov/factsheets/VitaminB6-HealthProfessional/
4. Dakshinamurti S, Dakshinamurti K (2007) Vitamin B6 in handbook of vitamins. In: Zempleni J, Rucker RB, McCormick DB, Suttie JW (Eds.), (4th edn), CRC Press, Taylor & Francis Group, Boca Raton, USA, pp. 315-360.
5. https://en.wikipedia.org/wiki/Pyridoxine
6. Aboul-Enein HY, Loutfy MA (1984) Pyridoxine hydrochloride in analytical profiles of drug substances. In: Florey K (Ed.), Academic Press Inc, Orlando, USA, 13: 448-478.
7. AlSaad D, Awaisu A, Elsalem S, Abdulrouf PV, Thomas B, et al. (2017) Is pyridoxine effective and safe for post-partum lactation inhibition? A systematic review. J Clin Pharm Ther 42(4): 373-382.
8. Pyridoxine Hydrochlorid (2016) The American society of health-system pharmacists.
9. Rubik B, Muehsam D, Hammerschlag R, Jain S (2015) Biofield science and healing: History, terminology, and concepts. Global Advances in Health and Medicine 4: 8-14.
10. Nemeth L (2008) Energy and biofield therapies in practice. Beginnings 28: 4-5.
11. Warber SL, Cornelio D, Straughn, J, Kile G (2004) Biofield energy healing from the inside. J Altern Complement Med 10(6): 1107-1113.
12. Movaffaghi Z, Farsi M (2009) Biofield therapies: Biophysical basis and biological regulations? Complement Ther Clin Pr 15(1): 35-37.
13. Sewitch MJ, Rajput Y (2010) A literature review of complementary and alternative medicine use by colorectal cancer patients. Complement Ther Clin Pr 16: 52-56.
14. Koithan M (2009) Introducing complementary and alternative therapies. J Nurse Pract 5: 18-20.
15. Trivedi MK, Mohan TRR (2016) Biofield energy signals, energy transmission and neutrinos. American Journal of Modern Physics 5: 172-176.
16. Trivedi MK, Mohan RR, Branton A, Trivedi D, Nayak G, et al. (2015) Evaluation of atomic, physical, and thermal properties of bismuth oxide powder: An impact of biofield energy treatment. American Journal of Nano Research and Applications 3: 94-98.
17. Trivedi MK, Tallapragada RM (2009) Effect of superconsciousness external energy on the atomic, crystalline and powder characteristics of carbon allotrope powders. Materials Research Innovations 13: 473-480.
18. Trivedi MK, Tallapragada RM, Branton A, Trivedi D, Nayak G, et al. (2015) Physicochemical characterization of biofield energy treated calcium carbonate powder. American Journal of Health Research. 3(6): 368-375.
19. Trivedi MK, Tallapragada RM, Branton A, Trivedi D, Nayak G, et al. (2015) Evaluation of biofield energy treatment on physical and thermal characteristics of selenium powder. Journal of Food and Nutrition Sciences. 3(6): 223-228.
20. Trivedi MK, Tallapragada RM, Branton A, Trivedi D, Nayak G, et al. (2015) The potential impact of biofield energy treatment on the physical and thermal properties of silver oxide powder. International Journal of Biomedical Science and Engineering 3(5): 62-68.
21. Trivedi MK, Patil S, Shettigar H, Bairwa K, Jana S (2015) Spectroscopic characterization of biofield treated metronidazole and tinidazole. Med chem 5(7): 340-344.
22. Trivedi MK, Branton A, Trivedi D, Nayak G, Panda P, et al. (2016) Determination of isotopic abundance of $^{13}C/^{12}C$ or $^2H/^1H$ and $^{18}O/^{16}O$ in biofield energy treated 1-chloro-3-nitrobenzene (3-CNB) using gas chromatography-mass spectrometry. Science Journal of Analytical Chemistry 4: 42-51.
23. Trivedi MK, Branton A, Trivedi D, Nayak G, Panda P, et al. (2016) Mass spectrometric analysis of isotopic abundance ratio in biofield energy treated thymol. Frontiers in Applied Chemistry 1(1): 1-8.

24. Trivedi MK, Branton A, Trivedi D, Nayak G, Mondal SC, et al. (2015) Antimicrobial sensitivity, biochemical characteristics and biotyping of *Staphylococcus saprophyticus*: An impact of biofield energy treatment. J Women's Health Care 4(6): 271.

25. Trivedi MK, Branton A, Trivedi D, Nayak G, Shettigar H, et al. (2015) Antibiogram of multidrug-resistant isolates of *Pseudomonas aeruginosa* after biofield treatment. J Infect Dis Ther 3: 244.

26. Trivedi MK, Branton A, Trivedi D, Nayak G, Mondal SC, et al. (2015) Evaluation of plant growth, yield and yield attributes of biofield energy treated mustard (*Brassica juncea*) and chickpea (*Cicer Arietinum*) seeds. Agriculture, Forestry and Fisheries. 4: 291-295.

27. Trivedi MK, Branton A, Trivedi D, Nayak G, Gangwar M, et al. (2015) Evaluation of vegetative growth parameters in biofield treated bottle gourd (*Lagenaria siceraria*) and okra (*Abelmoschus esculentus*). International Journal of Nutrition and Food Sciences. 4: 688-694.

28. Trivedi MK, Branton A, Trivedi D, Nayak G, Mondal SC, et al. (2015) Evaluation of plant growth regulator, immunity and DNA fingerprinting of biofield energy treated mustard seeds (*Brassica juncea*). Agriculture, Forestry and Fisheries. 4: 269-274.

29. Trivedi MK, Patil S, Shettigar H, Gangwar M, Jana S (2015) *In vitro* evaluation of biofield treatment on cancer biomarkers involved in endometrial and prostate cancer cell lines. J Cancer Sci Ther 7: 253-257.

30. Leklem JE (2001) Vitamin B6 in Handbook of Vitamins. In: Rucker RB, Suttie JW, McCormick DB, Machlin LJ (Eds.), (3rd edn), Marcel Dekker Inc, New York, USA, pp. 339-396.

31. Branton A, Jana S (2017) Evaluation of the effect of the energy of consciousness healing treatment on physicochemical and thermal properties of pyridoxine hydrochloride. American Journal of Physical Chemistry 6: 49-58.

32. Branton A, Jana S (2017) The influence of energy of consciousness healing treatment on low bioavailable resveratrol in male Sprague Dawley rats. International Journal of Clinical and Developmental Anatomy 3: 9-15.

33. Branton A, Jana S (2017) The use of novel and unique biofield energy healing treatment for the improvement of poorly bioavailable compound, berberine in male Sprague Dawley rats. American Journal of Clinical and Experimental Medicine 5: 138-144.

34. Branton A, Jana S (2017) Effect of the biofield energy healing treatment on the pharmacokinetics of 25-hydroxyvitamin D_3 [25(OH)D_3] in rats after a single oral dose of vitamin D_3. American Journal of Pharmacology and Phytotherapy 2: 11-18.

35. Liu Q, Hintelmann H, Jiang G (2016) Natural stable isotopes: new tracers in environmental health studies. Natl Sci Rev 3: 410.

36. Wiederhold JG (2015) Metal stable isotope signatures as tracers in environmental geochemistry. Environ Sci Technol 3: 2606-2624.

37. Schellekens RC, Stellaard F, Woerdenbag HJ, Frijlink HW, Kosterink JG (2011) Applications of stable isotopes in clinical pharmacology. Br J Clin Pharmacol 72: 879-897.

38. Muccio Z, Jackson GP (2009) Isotope ratio mass spectrometry. Analyst 134: 213-222.

39. Weisel CP, Park S, Pyo H, Mohan K, Witz G (2003) Use of stable isotopically labeled benzene to evaluate environmental exposures. J Expo Anal Environ Epidemiol 13: 393-402.

40. http://www.ionsource.com/Card/Mass/mass.htm

41. https://chem.libretexts.org/Bookshelves/Analytical_Chemistry/Supplemental_Modules_(Analytical_Chemistry)/Instrumental_Analysis/Mass_Spectrometry/Mass_Spectrometry%3A_Isotope_Effects

42. Smith RM (2004) Understanding mass spectra: A basic approach. (2nd edn), John Wiley & Sons Inc, ISBN 0-471-42949-X.

43. Jürgen H (2004) Gross mass spectrometry: A textbook (2nd edn) Springer, Berlin, Germany.

44. Susanne M (2016) Direct neutrino mass experiments. Journal of Physics: Conference Series 718: 022013.

45. Nakamura K, Petcov ST (2016) Neutrino mass, mixing, and oscillations. Chin Phys 40: 100001.

46. Kajita T (2010) Atmospheric neutrinos and discovery of neutrino oscillations. Proceedings of the Japan Academy Series B, Physical and Biological Sciences 86(4): 303-321.

47. McDonald, AB (2015) The sudbury neutrino observatory: Observation of flavor change for solar neutrinos: Lecture slides Nobel Lecture, Aula Magna, Stockholm University, Sweden.

48. Kajita, T (2015) Discovery of atmospheric neutrino oscillations: lecture slides, Nobel lecture, Aula Magna, Stockholm University, Sweden.

49. Głowinkowski S, Peplińska B, Jurga S (2004) Molecular dynamics in solid pyridoxine as studied by ^{1}H NMR. Solid State Nuclear Magnetic Resonance 25: 1-4.

50. http://www.bmrb.wisc.edu/metabolomics/mol_summary/show_data.php?molName=Pyridoxine&id=bmse000288.